were derived using the analytic wave function of H. Shull and P.-O. Löwdin, J. Chem. Phys. 25, 1035 (1956).
[11]J. A. Strozier, Jr., thesis, University of Utah, 1966 (unpublished).
[12]T. L. Loucks and P. H. Cutler, Phys. Rev. 133, A819 (1964).
[13]J. B. Pendry, J. Phys. C: Proc. Phys. Soc., London 1, 1065 (1968).
[14]J. H. Tripp, P. M. Everett, W. L. Gordon, and R. W. Stark, Phys. Rev. 180, 669 (1969).
[15]B. I. Lundqvist, Phys. Status Solidi 32, 273 (1969).

LOCALIZATION IN DISORDERED MATERIALS: BINARY ALLOYS*

E. N. Economou, S. Kirkpatrick, Morrel H. Cohen, and T. P. Eggarter
James Franck Institute, University of Chicago, Chicago, Illinois 60637
(Received 13 July 1970)

A criterion for localization of electron states in disordered materials is presented. Applications to binary alloys, made using the self-energy calculated in the coherent-potential approximation, confirm the Mott-Cohen-Fritzsche-Ovshinsky model in detail. Mobility edges occur inside the band edges. A mobility gap can appear within the band. The band can split into sub-bands, each with mobility edges. Below a critical concentration, an Anderson transition, where the minority sub-band becomes entirely localized, can occur.

Considerable effort has recently been devoted to calculation of the densities of states in different disordered materials.[1-3] In particular, the case of substitutional disorder has been brought to a quantitative level of understanding of the density of states through the application of the coherent-potential approximation (CPA)[4] to binary alloys.[5] Nevertheless, understanding of the nature of the wave functions in disordered materials has remained at the qualitative level exemplified by the Mott-Cohen-Fritzsche-Ovshinsky (MCFO) model.[6,7] That model assumes the existence of regions of exclusively localized states separated by critical energies,[6] termed mobility edges,[7] from regions of exclusively extended states.

In a recent paper[8] based on Anderson's statistical approach,[9] the formal theory[9-12] supporting the MCFO model has been reviewed and extended to the point where it has been demonstrated that a function $F(E)$ exists such that $F<1$ in the regions of localized states, $F>1$ in the region of extended states, and $F(E_c)=1$ at the mobility edges E_c. Moreover, a significant step towards a quantitative determination of $F(E)$ has been taken by relating $F(E)$ to properties of the average Green's function. Using this relation one can easily prove that when the average Green's function is translationally invariant with a k-independent self-energy, $\Sigma(E)$, $F(E)$ is then given by

$$F(E)=\{\max_{\vec{k}}|E(\vec{k})|\}/|E-\Sigma(E)|, \qquad (1)$$

where $E(\vec{k})$ is the band structure corresponding to the average Hamiltonian. Formula (1) has already been applied[8] to the specific case of a Lorentzian distribution of single-site energies, and exact quantitative results have been obtained for E_c.

The first purpose of this paper is to present as a conjecture the generalization of criterion (1) to all disordered systems which are translationally invariant when averaged [so that the self-energy becomes diagonal in $\vec{k}$, $\Sigma=\Sigma(\vec{k},E)$]:

$$F(E)=\{\max_{\vec{k}}|E(\vec{k})|/|E-\Sigma(\vec{k},E)|\}. \qquad (2)$$

Second, we combine this criterion (1) with the approximate self-energies available through the CPA[13] to obtain quantitative predictions of the character of the eigenstates in binary alloys. The self-energy is k independent in the CPA. We may therefore use (1), and errors will arise only from inaccuracies in the CPA values for Σ. Such errors in Σ, on entering $F(E)$, have the effect only of shifting the values of E_c found; corresponding errors in a mobility calculation lead to finite mobilities within a region of states which are actually localized.

For the calculations reported in this Letter, we consider a binary substitutional alloy A_xB_{1-x} in which there is a single Wannier function associated with each site. In the Hamiltonian,

$$H=\sum_i|i\rangle\epsilon_i\langle i|+\sum_{i\neq j}|i\rangle V_{ij}\langle j|, \qquad (3)$$

the diagonal elements, ϵ_i, take on two values ϵ^A and ϵ^B, on A and B sites, respectively, while the off-diagonal elements are translationally invariant. We shall define a scattering strength,

$\delta = \epsilon^A - \epsilon^B$, which provides a measure of the disorder in the alloy. Because the averaged Green's function is translationally invariant we may calculate the density of states from its diagonal matrix elements on a single site:

$$\rho(E) = (-1/\pi N)\,\mathrm{Im\,Tr}\,\langle G(E+i0)\rangle_{\mathrm{av}}$$

$$= (-1/\pi)\,\mathrm{Im}\,\langle 0|\langle G(E+i0)\rangle_{\mathrm{av}}|0\rangle. \qquad (4)$$

Equation (4) permits the calculation of the average density of states on A or on B sites in the alloy merely by restricting the site $|0\rangle$ to contain an A or B atom. In this way partial densities of states ρ^A and ρ^B are defined[5] such that

$$\rho(E) = x\rho^A(E) + (1-x)\rho^B(E), \qquad (5)$$

and $n^A(E)$, the fractional A parentage of the states at energy E, is defined by $n^A(E) = x\rho^A(E)/\rho(E)$.

In the CPA, knowledge of the off-diagonal matrix elements of (3) can be replaced by the specification of the density of states in the unperturbed case $\epsilon^A = \epsilon^B = 0$. Except when otherwise stated, the calculations in this Letter were performed on the semicircular model for the density of states.[5] We take the A components to be in the minority, and $\epsilon^A > \epsilon^B$. $E(\vec{k})$ is symmetric and $\max_k[E(\vec{k})] = 1$.

Most of the behavior observed in the model is exhibited in Fig. 1, the four sections of which show the alloy density of states for $x = 0.1$ and four values of δ, increasing from bottom to top. Also plotted with each section of the figure are the localization function $F(E)$ and the parentage $n^A(E)$. Mobility edges, indicated by arrows labeled E_c, are found inside both band edges at all values of the scattering strength, moving farther in as δ is increased. In Fig. 1(b) a mobility gap, a region of localized states surrounded on both sides by extended states, like that hypotheized by Mott,[6] has formed with the band. As δ is increased [Fig. 1(c)], an impurity sub-band is drawn off. Mobility edges are observed at the top and bottom of both sub-bands. Finally, for still larger δ, shown in Fig. 1(d), the states in the impurity sub-band are all localized.

From the quantities plotted in Fig. 1 we can assemble a detailed interpretation of the behavior of the model system (3). The different features are best resolved in Fig. 1(c), where four regions of localization and two of extended states can be seen, each region corresponding to wave functions of different character. We shall discuss first the states in the majority sub-band. Both mobility edges lie very close to the edges of the CPA density of states for this sub-band. The states in the lower region are isolated on large islands of pure B material. The extended states percolate through connected regions of mostly B. At energies above the upper mobility edge, the percolation regions are channels which have been interrupted by fluctuations of higher A content. All this is reflected in the very low values of the A parentage through most of the sub-band, and its steep rise at the upper mobility edge.

We expect the positions of the mobility edges predicted from the CPA to be a fair approximation to the true mobility edges, especially in the majority sub-bands, because they are approached from the region of extended states, the only region in which the effective medium approximation is well founded. This argument also explains why the true band edges cannot be found accurate-

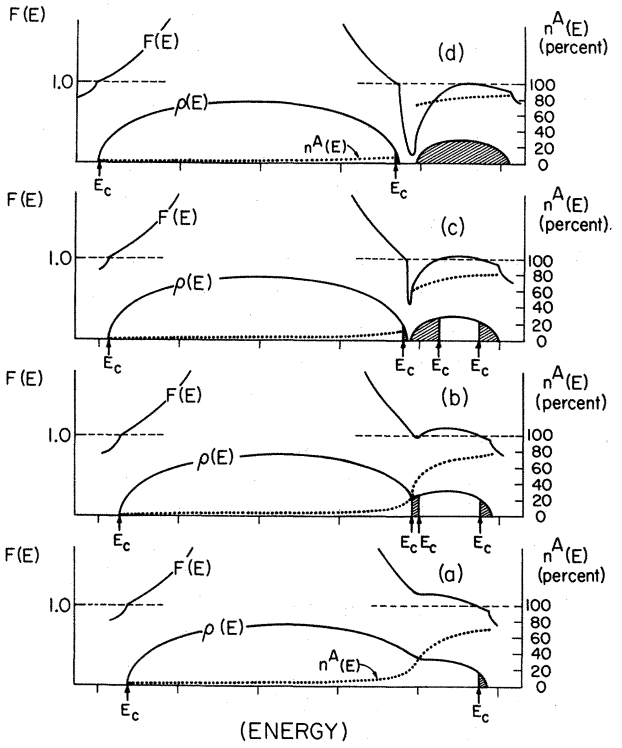

FIG. 1. Alloy density of states (in arbitrary units) and properties related to localization, calculated by the CPA for the model Hamiltonian (3) with $x = 0.1$, and δ = (a) 0.7, (b) 0.8, (c) 0.95, and (d) 1.1. Regions of localized states have been shaded. The heavy line above each density of states indicates the localization function $F(E)$ defined by (1); the dotted line the A parentage $n^A(E)$ defined in the text.

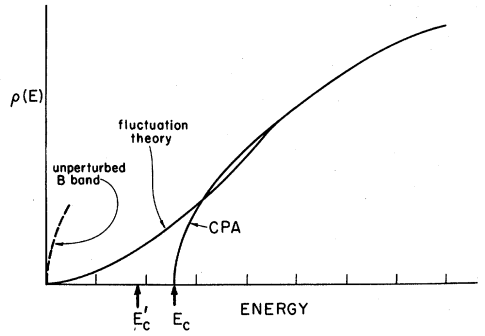

FIG. 2. Tail of the density of states, as calculated from the fluctuation theory, compared with the CPA result for $x = 0.1$, $\delta = 0.5$. E_c denotes the mobility edge predicted from the CPA and (1), and E_c'' the fluctuation. E_c' and E_c differ by 0.004 times the unperturbed B band width.

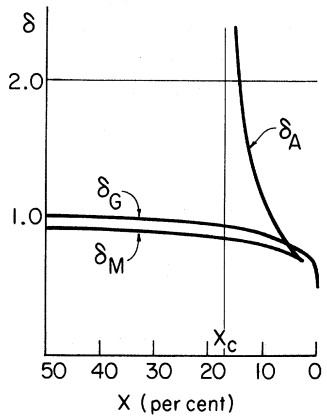

FIG. 3. Phase diagram of the alloy model (3), as obtained from the CPA self-energy. δ_M denotes the critical value of δ for the appearance of a mobility gap at a given concentration, δ_G the opening of a gap in the density of states, and δ_A the Anderson transition for the impurity states. The concentration above which the Anderson transition no longer takes place is denoted x_c. The exact limiting behavior for δ_G is indicated by the light line at $\delta = 2$.

ly from the CPA. To study band-edge states outside the mobility edges, we have used a different procedure, possible only near the lower band edge. This procedure, an application of the ideas introduced by Eggarter and Cohen,[14] is a semiclassical calculation of scattering from fluctuations of the impurity concentration. The details of this calculation will be published elsewhere.

The tail in the density of states obtained from the fluctuation calculation and its mobility edge (E_c) are plotted against the CPA results in Fig. 2, for the case $x = 0.1$, $\delta = 0.5$. This figure should typify the behavior to be found at the other CPA band edges. The mobility edges obtained by the two methods are in rough agreement, but the lower band edges are not, as was expected, a result true for all δ at the low concentrations for which the fluctuation calculation is valid. The new lower band edge in Fig. 2 occurs at the energy of the largest possible fluctuation, i.e., the bottom of the unperturbed B band structure, as first suggested by Lifshitz.[1]

The minority states of Fig. 1 can be assigned to three categories, associated with the three regions of the minority sub-band in Fig. 1(c). At the highest energies are states localized on isolated islands of A sites, while the extended impurity states at slightly lower energies are associated with channels of mostly A atoms. $F(E)$ for these extended states is never much greater than 1, suggesting that the associated wave functions are highly constricted. This is in sharp contrast to the situation for the extended majority states, for most of which $F(E) \gg 1$. The localized states just above the gap in Figs. 1(c) and 1(d) [and at the top of the mobility gap in Fig. 1(b)] are those in which the channels have been blocked by fluctuations of high local B concentration. The parentage n^A calculated in the CPA is consistent with this interpretation. In Fig. 1(c) it rises sharply from 25 to 50% in crossing the mobility gap. At the top of the band, n^A has risen to 7-9 times the impurity concentration.

The sequence of events seen in Fig. 1 furnishes an operational definition of an Anderson[9] transition as the disappearance of a region of extended states through the merging of two mobility edges. Thus, at a given concentration we may define a critical value of δ, δ_M, at which the mobility gap first appears [Fig. 1(b)], another, δ_G, for the appearance of a gap in the density of states [Fig. 1(c)], and a third, δ_A, at which the Anderson transition occurs for the minority states [Fig. 1(d)]. These critical values of δ, as obtained from the CPA self-energy, are plotted as functions of x in Fig. 3. For concentrations greater than a critical value x_c, no Anderson transition occurs, and there are extended states in both sub-bands as $\delta \to \infty$.

The lines representing δ_A and δ_M meet and are terminated at a concentration slightly less than 3% because at lower x the localization region extending down from the top of the band fills the region associated with the impurity states before a mobility gap can form. The operational definitions of δ_M and δ_A given above can then no longer be applied.

The "phase diagram" comparable with Fig. 3 which describes the exact solution to the model alloy (3) should differ only quantitatively from Fig. 3. We do not expect the exact δ_M to be very different from that plotted here, as was explained above. The asymptote for δ_A will, as discussed below, occur at a larger value of x_c than we have calculated with the CPA, but the character of the line will be the same. However, an exact calculation for the Hamiltonian (3) would give a spectrum with a true gap and two distinct allowed regions only when the spectra obtained by setting all the $\epsilon_i = \epsilon^A$ and that obtained by setting them all equal to ϵ^B do not overlap.[1,15] This criterion, concentration independent, requires $\delta_G = 2$ and is indicated by a light line in Fig. 3. The values of δ_G obtained with the CPA differ so much from 2 because the CPA gap, between sub-bands of extended states, is actually, as is evident from Fig. 3 and was discussed before (Fig. 2), very close to the mobility gap.

To calculate the critical concentration x_c, and some overall features of the states in a strongly split sub-band, we must establish a connection between the model (3) and percolation theory.[16] If the off-diagonal terms in (3) contain nearest-neighbor hopping only, and if the bandwidth can be neglected with respect to δ, then an electron can escape a given A site only if it has an A neighbor. Finding the relative number of extended states in the whole sub-band at a concentration x is equivalent in this limit to the classical percolation problem of determining the likelihood that a particular site in a lattice lies on an infinite path of A's when the A's are distributed at random with probability x. This quantity, $P^A(x)$, has been calculated numerically for several three-dimensional lattices by Frisch et al.[17] In each case they find a sudden onset of percolation at a concentration p_c which depends upon Z, the number of nearest neighbors, approximately as $p_c = 1.8/Z$.

To test these results in the strong scattering limit, it is necessary to use a model density of states which corresponds to a definite Hamiltonian. We chose the case of a simple-cubic lattice with only nearest-neighbor overlap. The critical concentration obtained from CPA is only 12% (percolation theory gives 30%), but the fraction of extended states as a function of concentration appears in all other respects as if the percolation probability for the simple-cubic lattice had been shifted to the new origin. This suggests, therefore, that the extended states predicted in the strong scattering limit do have the expected percolation character. The CPA self-energy has the effect of magnifying the number of effective nearest neighbors, i.e., of underemphasizing the randomness in the way it replaces the potential on each site by an effective potential.

In this Letter we have made use of the proposed criterion (1) to identify regions of localized states in a simple model of a binary substitutional alloy, using the averaged Green's function calculated in the CPA. Both the quantitative results for this model and the qualitative behavior which the model typifies are of considerable interest and novelty. A striking confirmation of the MCFO model is obtained.

The overall picture that emerges, when combined with independent calculations and estimates of particular aspects, supports the correctness of our approach. Because the procedure is so simple to apply, and the results already obtained by its use with the CPA are so rich, it should prove a valuable tool for evaluating proposed extensions of the CPA,[18] which promise better calculations of the averaged Green's function, especially in the strong-scattering limit and in the tails, as well as an incentive for continuing with such extensions.

---

*Work supported by the Army Research Office (Durham), The National Aeronautics and Space Administration, and the Advanced Research Projects Agency.

[1]I. M. Lifshitz, Usp. Fiz. Nauk 83, 617 (1964) [Sov. Phys.—Usp. 7, 549 (1965)].

[2]B. I. Halperin and M. Lax, Phys. Rev. 148, 722 (1966).

[3]S. F. Edwards, Proc. Roy. Soc., Ser. A 267, 518 (1962).

[4]P. Soven, Phys. Rev. 156, 809 (1967).

[5]B. Velický, S. Kirkpatrick, and H. Ehrenreich, Phys. Rev. 175, 747 (1968).

[6]N. F. Mott, Advan. Phys. 16, 49 (1967).

[7]M. H. Cohen, H. Fritzsche, and S. R. Ovshinsky, Phys. Rev. Lett. 22, 1065 (1969); M. H. Cohen, to be published.

[8]E. N. Economou and M. H. Cohen, to be published.

[9]P. W. Anderson, Phys. Rev. 109, 1492 (1958).

[10]N. F. Mott, to be published.

[11]J. M. Ziman, J. Phys. C: Proc. Phys. Soc., London 2, 1230 (1969).

[12]D. J. Thouless, to be published.

[13]However, it can be shown that the CPA calculation of the self-energy is exact in the Lorentzian model treated in Ref. 8.

[14]T. P. Eggarter and Morrel H. Cohen, to be published.

[15]For a simple proof that this is a sufficient condition, see S. Kirkpatrick, B. Velický, and H. Ehrenreich,

Phys. Rev. B 1, 3250 (1970), Appendix B.
[16]S. R. Broadbent and J. M. Hammersley, Proc. Cambridge Phil. Soc. 53, 629 (1957).
[17]H. L. Frisch, J. M. Hammersley, and D. J. A. Welsh, Phys. Rev. 126, 949 (1962).
[18]K. Freed and M. H. Cohen, to be publsihed.

CRYSTAL FIELDS AND THE MAGNETIC PROPERTIES OF PRASEODYMIUM AND NEODYMIUM

T. Johansson
Technical University, Lyngby, Denmark

and

B. Lebech, M. Nielsen, and H. Bjerrum Møller
Atomenergikommissionen Research Establishment, Risø, Denmark

and

A. R. Mackintosh
H. C. Ørsted Institute, University of Copenhagen, Denmark
(Received 29 June 1970)

The magnetic properties of Pr and Nd single crystals have been studied by neutron-diffraction and susceptibility measurements. In contrast to earlier results on polycrystals, monocrystalline Pr is found not to be magnetically ordered, because of crystal field effects, but a magnetic field induces a large moment. Anisotropic effective exchange results in a large magnetic anisotropy. The complex magnetic structure of Nd is substantially modified by a magnetic field.

The magnetic properties of the light rare-earth metals Pr and Nd are of particular interest because the crystal-field splittings of the magnetic energy levels in the double-hexagonal-close-packed (dhcp) structure are comparable with the exchange energies. This is in contrast to, for instance, the heavy rare earths, where the crystal field acts as a source of magnetic anisotropy which, though relatively strong, is still small compared with the exchange. We have investigated these crystal-field effects in single crystals by neutron-diffraction experiments in fields as large as 50 kG, and through magnetic susceptibility measurements by the Faraday method.

The dhcp structure consists of two inequivalent sets of ionic sites, one of which is in a local environment with hexagonal symmetry and the other with cubic symmetry. The crystal-field energy levels in Pr have been considered by Bleaney[1] who showed that the ground states of the ions at both types of site are singlets; thus, magnetic ordering will not occur unless the ratio of exchange to crystal-field interactions exceeds a critical value.[2] On the assumption that no magnetic ordering actually occurs in Pr, he calculated a number of properties, including the magnetic susceptibility. Systems with crystal-field singlet ground states have been extensively discussed by Wang and Cooper.[3] Cable et al.[4] showed by neutron diffraction that a polycrystalline sample of Pr was antiferromagnetic with a Néel temperature of about 25°K, and suggested that only the hexagonal sites order. We observed no trace of spontaneous magnetic ordering in a single crystal of Pr at 4.2°K. Since the occurrence of antiferromagnetism in a polycrystalline sample and its absence in a monocrystal has also been observed by Rainford and Wedgwood,[5] we conclude that pure monocrystalline Pr is not antiferromagnetic but that the exchange is sufficiently great that a small modification of the crystal-field splittings, perhaps due to strains, can lead to spontaneous ordering.

The application of a magnetic field along the $\vec{b}_2$ (110) direction produces a large induced moment, which shows a substantial tendency towards saturation at high fields and low temperatures, as shown in Fig. 1. By observing the neutron-diffraction intensities at different reciprocal-lattice points, it is possible to separate the contributions from the cubic and hexagonal sites; we find that μ(hexagonal) = $1.8\mu_B$/ion while μ(cubic) = $0.9\mu_B$/ion at 4.2°K and 46 kG. A fairly good fit to these results may be obtained[5] using a molecular-field model and the crystal-field level scheme deduced by Bleaney,[1] except that the best value for the energy separation between the ground state and the first-excited doublet